RSC Advances

PAPER

View Article Online
View Journal | View Issue

Cite this: *RSC Adv.*, 2020, **10**, 32953

Lipoic acid capped silver nanoparticles: a facile route to covalent protein capping and oxidative stability within biological systems†

Irene Guzmán-Soto,[a] Mary Omole,[a] Emilio I. Alarcon *[ab] and Christopher D. McTiernan *[a]

Received 17th August 2020
Accepted 27th August 2020

DOI: 10.1039/d0ra07080g

rsc.li/rsc-advances

Covalent attachment of human serum albumin protein to the surface of spherical lipoic acid capped silver nanoparticles results in the generation of stable nanoparticle–protein hybrids with well defined surface composition. Enhanced stability towards oxidation and in the presence of complex media with high ionic strength, holds promise towards the use of these conjugates as therapeutics in biomedical applications and sensing.

Introduction

The development of novel nanoparticle-based therapeutics for biomedical applications rely on the ability to generate stable particles that present well defined surfaces to their biological surroundings. While silver nanoparticles (AgNPs) have been demonstrated to display broad spectrum antibacterial effects,[1,2] anti-inflammatory properties,[3] and an ability to inhibit biofilm formation;[4,5] these characteristics are dependent on the size, shape, and nature of the capping agent.[6] Furthermore, it is well documented that the fate and biological activity of AgNPs within living systems are highly dependent on the functionalities presented by the particles (*e.g.* capping/surface groups) as this is what these systems interact with.[1,7] While various molecules have been used to cap or protect the surface of AgNPs, not all of these are created equally, with some displaying stronger interactions than others. In the case of weakly adsorbing capping agents, the surface composition of the nanoparticles in biological media is quite dynamic with passive adsorption of proteins and other large biomacromolecules steering the composition of the protein corona *via* an equilibrium-controlled process.[8–10] Considering that such dynamic alterations can result in drastic changes in the properties and function of the nanoparticle, it is important that such modifications are limited. One such way to limit these changes is to utilize capping agents with higher affinities for the surface of the noble metals than the proteins which are found within biological fluids.

Recently, our group reported that nanoparticle–protein systems comprised of spherical AgNPs and a physically adsorbed protein corona of human serum albumin (HSA) display enhanced stability towards peroxyl radical oxidation, with the resulting composites being less prone to oxidation than either of its individual components.[11] While this result is promising towards the goal of generating stable protein–nanoparticle composites, due to the non-covalent nature of the interaction between HSA and the AgNPs surface, predictability of the protein corona composition remains an issue upon addition of the composite to complex biological media. As such we set out to bioconjugate the HSA protein to the surface of the AgNPs.

A thiol containing capping agent that has found widespread use in the development of metal nanoparticle bioconjugates is lipoic acid (LA), also referred to as thioctic acid. LA is a 5-membered cyclic disulphide compound with a 5-carbon tail/spacer and terminal carboxylic acid group. It has been demonstrated to have both antioxidant and anti-inflammatory properties,[12] and presents dual anchoring groups,[13] which strengthen its interaction with noble metal surfaces such as Au, Cu and Ag.[14,15] Furthermore, the terminal carboxylic acid is a prime orthogonal handle through which a variety of molecules can be chemically tethered. While there are several reports regarding the preparation and/or application of LA capped AgNPs; there is little agreement regarding the properties of these conjugates,[16–28] and while most of these differences are likely traced backed to differences within the protocols used to prepare the nanoparticles (*i.e.* chemical, photochemical, with and without surfactant, concentrations), it is important to note that not all AgNPs are equivalent, with characteristics such as size, shape, and initial capping agent all having a strong influence on the resulting particles even after exchange.

Nevertheless, there are reports of LA capped silver nanoparticles being less toxic than uncapped or polyethylene glycol (PEG) capped AgNPs,[19] and that surface bound LA retains some

[a]*Division of Cardiac Surgery, University of Ottawa Heart Institute, 40 Ruskin Street, Ottawa, Canada. E-mail: ealarcon@ottawaheart.ca; cmctiernan@ottawaheart.ca*

[b]*Department of Biochemistry, Microbiology, and Immunology, Faculty of Medicine, University of Ottawa, Ottawa, Canada*

† Electronic supplementary information (ESI) available. See DOI: 10.1039/d0ra07080g

ability to scavenge radicals, albeit with less efficiency than free LA.[23] Thus, exploitation of the carboxyl functionality of LA to tether proteins, such as HSA, would appear to be an ideal route to stable protein–AgNP conjugates.

Herein, we explore the preparation and characterization of conjugated HSA AgNPs from LA capped AgNPs, which were obtained through capping agent exchange of photochemically prepared citrate capped AgNPs. Through examination of the resulting particle stability in solutions of high ionic strength, relevant biological media, and the presence of reactive oxygen species (ROS), we hope to illustrate that chemical tethering of HSA to the surface of AgNPs *via* LA linker is a viable route to well-defined nanostructures of biological relevance, while highlighting properties which could be exploited in future applications.

Results and discussion

The preparation of LA capped AgNPs was accomplished through the capping agent exchange of photochemically prepared citrate capped AgNPs (roughly 3–5 nm diameter) through incubation in solutions of various LA concentrations over a 24 h period (see Scheme 1 and Fig. 1).

Upon addition of aqueous solutions of LA in concentrations ranging from 2.5–100 μM to spherical citrate capped AgNP (80 nM nominal concentration) there was an apparent red shift in the absorption of the nanoparticle solution over a period of 24 h. As seen in Fig. 1A at concentrations above 5.0 μM LA this colour change can be explained through the appearance of a new secondary absorption maximum centred around 515–530 nm. The appearance of this new absorption is likely the result of aggregation of the AgNPs, which is in good agreement with the dynamic light scattering (DLS) and transmission electron microscope (TEM) measurements, Fig. 1B and F respectively, which show an increase in average hydrodynamic size and particle diameter with increasing concentrations of LA.

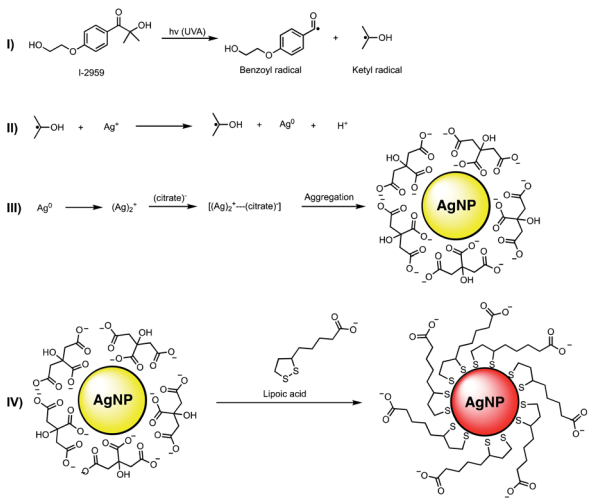

Scheme 1 Preparation of LA functionalized AgNPs from photochemically prepared citrate capped AgNPs.

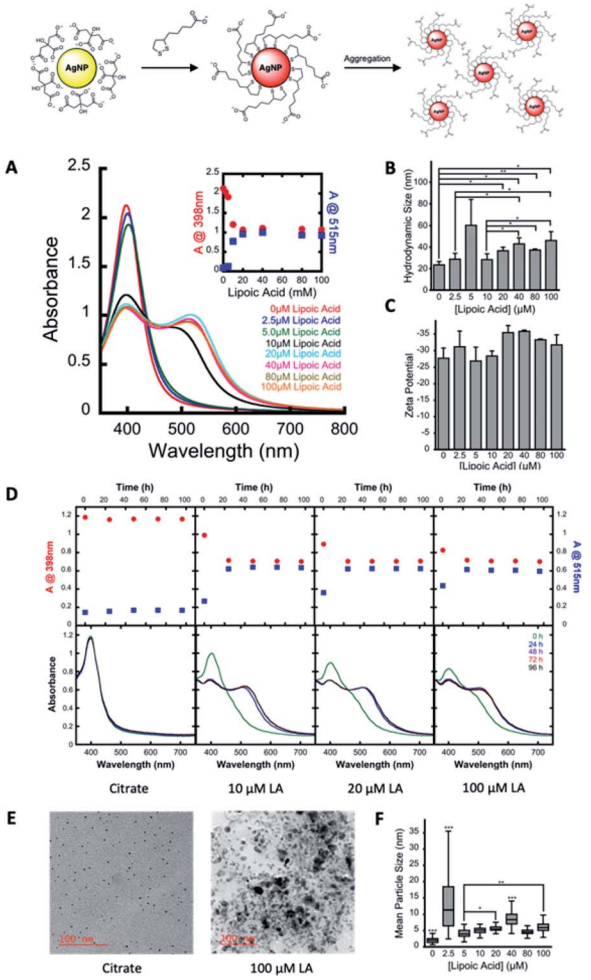

Fig. 1 Preparation and characterization of LA capped AgNP. (A) UV-vis absorption spectra of photochemically prepared citrate capped AgNP 24 h after the addition of increasing concentrations of LA. Inset: decrease and increase in absorption at 398 nm and 515 nm of AgNP solutions measured 24 h after addition of various LA concentrations. (B) Hydrodynamic size measured *via* dynamic light scattering of citrate capped AgNP 24 h after addition of various LA concentrations. (C) Zeta potential of citrate capped AgNP 24 h after addition of various LA concentrations. (D) Changes in absorption spectrum of LA capped AgNP as measured over a 96 h period. (E) TEM images of photochemically prepared citrate capped AgNP before and 24 h after the addition of 100 μM LA. (F) Mean particle size of AgNP measured from TEM images (>100 particles measured for each samples). *P*-Values * ≤ 0.05, ** ≤ 0.005 and *** ≤ 0.001 calculated from *t*-test Student.

Similar red shifts have also been observed in the preparation of LA capped AgNPs by other methods and attributed to particle aggregation;[21] however there are some reports showing that this induced aggregation may be the result of the chelation of superfluous metal cations by the negatively charged carboxyl groups of the LA.[20] Further, as the original surface plasmon band of the AgNP centred around 400 nm only decreases and does not disappear with the appearance of the new band at 530 nm (Fig. 1A and inset) it is likely that there is some intrinsic coupling of the two modes, which is further highlighted by the fact that the magnitude of the observed decrease in absorption

at 398 nm is the same as the observed increase in absorption at 515 nm for all concentrations of LA. Stability and zeta potential analysis also reveal that while aggregated, the particles remain stable colloids over a period of at least 96 h and present negatively charged surfaces that stabilize the dispersion. The stable LA capped AgNPs were then covalently functionalized with HSA as depicted in Fig. 2A. Amide bonds were generated between the primary amines of the HSA (59 lysine residues per HSA molecule – 66 kDa) and the carboxyl groups of the LA capping agent. This requires activation of the carboxylic acid utilizing 1-ethyl-3-(3-dimethylaminopropyl)carbodiimide (EDC) and *N*-hydroxysulfosuccinimide (Sulfo-NHS), *via* an *o*-acylisourea intermediate and subsequent succinimide ester. While attempts were made to functionalize the particles utilizing the non-sulfonated analogue of NHS, the resulting particles were not as stable due to the fact that the ester intermediate bears no charge thus resulting in a destabilization of the colloidal suspension and a decreased coupling efficiency. The Sulfo-NHS intermediate, on the other hand presents negatively charged sulfonate groups which stabilize the particles allowing for an increase in the coupling efficiency. While AgNPs capped with concentrations >10 μM LA all give rise to particles with similar characteristics, those capped with 100 μM LA appear to reach an equilibrium much quicker and as such we moved forward with the 100 μM LA AgNPs. Upon functionalization with HSA, the particles remained stable in solution, presented a broad absorption spectrum that spanned the entire visible spectrum, exhibited IR signals characteristic of HSA, and a slightly smaller average size of 5.44 nm than their corresponding LA AgNP (6.11 nm) as measured from TEM images of the functionalized particles (see Fig. 2), a characteristic likely due to redispersion of the nanoparticles upon addition of HSA. The functionalization of the particles was further confirmed through gel electrophoresis analysis of the conjugates, in which the HSA capped AgNP displayed a single band consistent with the formation of a conjugate considerably larger (MW > 170 kDa) than native HSA (MW 66 kDa) (see Fig. S1†) and not consistent with dimerization. The HSA capped AgNP also showed exceptional stability in the presence of 150 mM NaCl over an 8 h period and were also shown to be relatively stable in cell culture media (1× DMEM high – no phenol red) under optimized conditions (Fig. 2E and F), in comparison to the citrate AgNP that agglomerated under both conditions, losing much their absorbance at 400 nm immediately upon addition.

Next, we explored the stability of the prepared AgNP conjugates in the presence of reactive oxygen species (ROS) such as oxidizing peroxyl radicals. Considering that the eventual goal is to employ these particles within biological systems for the treatment of diseases it is important to understand whether or not these particles can withstand the oxidative stress which usually characterizes these environments. While peroxyl radicals are not the only ROS present in biological systems they are the radicals primarily responsible for protein and lipid oxidation.[29] Furthermore, we have previously demonstrated that AgNPs with physically adsorbed HSA protein coronas are relatively stable, undergo limited oxidation and result in increased generation of peroxides,[11] which could possibly be beneficial in the generation of antibacterial treatments or in therapies that rely on the generation of oxidative species (*i.e.* chemotherapy). Peroxyl radicals were generated at a steady rate from the thermal decomposition of 2,2′-azobis(2-methylpropionamidine)dihydrochloride (AAPH, 14 nM s^{-1} at 37 °C, see Fig. 3A).[30] By following the decrease in absorption of AgNP solutions at 400 nm as a function of time in the presence of 10 mM AAPH at 37 °C (see Fig. 3B), we were able to conclude that both LA and HSA capped particles, show enhanced stability in comparison to citrate capped AgNPs, with the HSA capped AgNPs generating approximately 2.2× more peroxides during the oxidation process than that observed for LA capped AgNPs and oxidized HSA solutions (see Fig. 3C). This is in good agreement with what we have previously observed with AgNPs with physically adsorbed HSA proteins coronas.[11] The advantage here is that the covalently tethered HSA is not prone to displacement by other species found within the biological system and is also not affected by changes

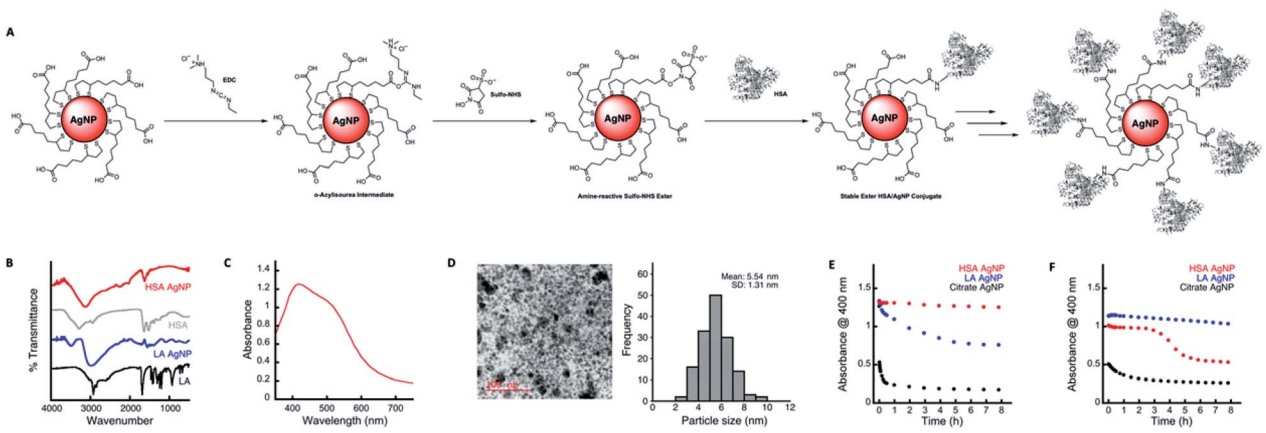

Fig. 2 Preparation and characterization of HSA capped AgNPs *via* EDC/Sulfo-NHS coupling. (A) Route to HSA capped AgNPs *via* LA capped AgNPs and EDC/Sulfo-NHS coupling. (B) IR spectrum of HSA capped AgNPs as compared to LA capped AgNPs and free HSA and LA. (C) UV-vis spectrum of HSA capped AgNPs. (D) TEM image of HSA capped AgNPs and corresponding size histogram. (E) Stability of HSA capped AgNPs in 150 mM NaCl. (F) Stability of HSA capped AgNPs in 1× DMEM high without phenol red (1 : 3 – media : AgNP).

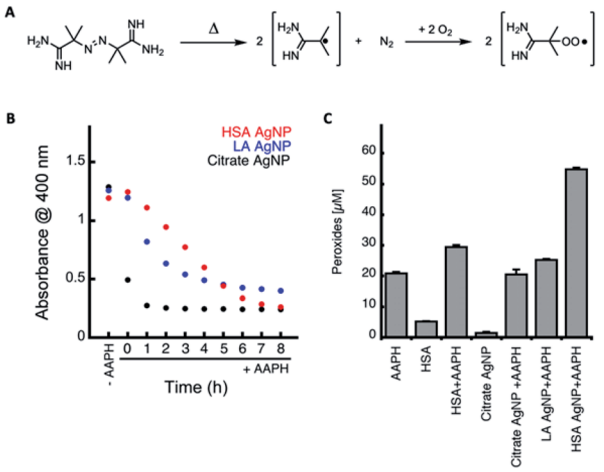

Fig. 3 Effects of peroxyl radicals on the stability of AgNP solutions. (A) Generation of peroxyl radicals through the thermal decomposition of AAPH in the presence of oxygen. (B) Change in absorption of various matched AgNPs solutions in the presence of 10 mM AAPH as a function of time as measured at 400 nm and 37 °C. −AAPH corresponds to *A* @ 400 nm before addition of AAPH, +AAPH corresponds to *A* @ 400 nm after addition of AAPH. (C) Concentration (μM) of peroxides formed upon AAPH mediated oxidation of various AgNPs solutions at 37 °C. Solutions consisted of AgNPs, 10 μM HSA, and 10 μM AAPH. Peroxides quantified spectrophotometrically using a Pierce quantitative peroxide assay kit.

in ionic strength. As such the covalent attachment of HSA to the surface of AgNPs *via* LA linker allows for the generation of structures whose properties and effects can be better predicted in complex biological media, where there exist a number of biomacromolecules that present functionalities known to bind efficiently to the surface of AgNPs.

Conclusions

In summary, we have prepared and characterized bioconjugated HSA AgNPs from LA capped AgNPs, which were obtained through capping agent exchange of photochemically prepared citrate capped AgNPs. By characterizing the stability of the resulting conjugate in solutions of high ionic strength, biologically relevant media, and highly oxidizing environments, we demonstrated that covalent tethering of HSA to the surface of AgNPs *via* LA linker is a viable route to well-defined nanostructures of biological relevance. Furthermore, due to the enhancement of peroxide formation in oxidative environments, it is easy to envision these particles finding roles as additives with synergistic effects in both antibacterial and chemotherapeutic applications.

Experimental section

Chemicals and reagents

Silver nitrate ($AgNO_3$), trisodium citrate, 2-hydroxy-1-[4-(2-hydroxyethoxy)phenyl]-2-methyl-1-propanone (I-2959), human serum albumin (HSA), 2,2′-azobis(2-methylpropionamidine) dihydrochloride (AAPH), sodium chloride (NaCl), lipoic acid (LA), 1-ethyl-3-(3-dimethylaminopropyl)carbodiimide (EDC) and *N*-hydroxysulfosuccinimide (Sulfo-NHS) were purchased and used as received from Sigma-Aldrich. All solutions were prepared using Milli-Q water.

Synthesis of citrate capped AgNPs

Citrate capped AgNPs were prepared by deoxygenation (30 min N_2) of an aqueous solution containing 0.2 mM $AgNO_3$, 0.2 mM I-2959, and 1.0 mM sodium citrate followed by irradiation with UVA light (8 lamps, in a Luzchem LZC-4 photoreactor at 25.0 ± 0.5 °C) for 30 min. Yellow translucent solutions were obtained in all cases and the solutions were kept at room temperature protected from light.

Preparation of LA capped AgNPs from citrate capped AgNPs

The citrate capped AgNPs were aliquoted as 1 mL samples into 1.5 mL Eppendorf tubes. A stock solution of 1 mM aqueous LA was prepared. Varying proportions of 1 mM LA and water were added to the citrate capped AgNP to give a total volume of 1.1 mL and concentrations ranging from 0–100 μM LA. The tubes were gently vortexed and then stored in the dark at room temperature for at least 24 h.

Functionalization of LA capped AgNPs with HSA

HSA was conjugated to LA utilizing EDC and Sulfo-NHS. Briefly, 6 × 1.5 mL eppendorfs containing LA capped AgNPs which were aged for at least 24 h were centrifuged for 30 minutes at 13 400 rpm. The supernatant was then decanted and the pellets of the 6 tubes combined (this gives approximately 60 μL of concentrated LA capped AgNP). Solutions comprising 30 mg mL^{-1} EDC and 60 mg mL^{-1} Sulfo-NHS in 0.1 M MES buffer were prepared and stored on ice. 30 μL of EDC solution was then mixed with 30 μL of Sulfo-NHS and then added to the 60 μL of concentrated LA capped AgNPs. The reaction was allowed to proceed at room temperature for 30 minutes. 1 mL of PBS-T was added, mixed, and then centrifuged for 10 minutes at 13 400 rpm. The supernatant was then discarded and 60 μL of 1 mg mL^{-1} HSA in 1× PBS was added and briefly sonicated to resuspend the particles. The reaction was allowed to proceed at room temperature for 1 hour, at which point 1 mL of PBS-T was added, mixed and centrifuged for 10 minutes at 13 400 rpm. This was repeated 3 × to remove any unbound HSA. After the final wash the particles were resuspended in 250 μL of 1× PBS with slight sonication and stored in the dark at 4 °C.

UV-vis spectra and kinetics measurements

The spectra and single wavelength absorption measurements were recorded at room temperature of 37 °C in a Spectra Max M2e (Molecular Devices) cuvette and microplate reader. Kinetics were performed following the absorption maximum of each sample.

Hydrodynamic size and zeta potential measurements

Hydrodynamic sizes and zeta potential measurements of the prepared AgNPs solutions were carried out in a Malvern

Zetasizer Nano ZS at 20 °C in 1.0 cm pathlength disposable plastic cuvettes. Values correspond to the average of three independent measurements.

Transmission electron microscopy (TEM) of AgNPs

Samples for TEM were prepared by delivering 10 μL of AgNPs solution on Formvar coated copper–carbon grids (400 mesh) and then dried under vacuum for 72 h before imaging. Electron microscopy images were obtained using a FEI Tecnai G2 F20 TEM operating with an acceleration voltage of 75 kV.

IR spectra of capping agents and AgNPs

IR spectra were recorded using an iD7 ATR accessory and a Nicolet iS5 Spectrometer (ThermoFisher). 200 scans per sample.

Stability in NaCl (high ionic strength)

The stability of AgNPs in 150 mM NaCl was measured by monitoring changes in the absorption spectrum as a function of time over 8 hours. Initially the absorption of all solutions were matched at 400 nm. All samples were ran in triplicate.

Stability in media

The stability of AgNPs in DMEM media without phenol red (HyClone cat. no. SH30284.01) was measured by monitoring changes in the absorption spectrum as a function of time over 8 hours. Initially the absorption of all solutions were matched at 400 nm. All samples were ran in triplicate.

Stability in the presence of AAPH

The absorption of the AgNPs solutions were matched at 400 nm in a 96 well plate. 10 mM AAPH was added to the wells and the decrease in absorption of the samples at 400 nm was measured as a function of time over a period of 8 h. Heating the samples to 37 °C resulted in thermal decomposition of AAPH and the generation of peroxyl radicals.

Peroxide quantification

The concentration of peroxides formed upon AAPH/peroxyl radical mediated oxidation of AgNPs solutions was performed using a Pierce quantitative peroxide assay kit (Thermo Scientific, USA). This kit works through the oxidation of ferrous to ferric ions in the presence of xylenol orange. Absorbance of the resulting purple solutions we measured in a SpectraMax M2e (Molecular Devices) plate reader at a wavelength of 595 nm.

Conflicts of interest

There are no conflicts to declare.

Acknowledgements

This work was supported by the Natural Sciences and Research Council of Canada (NSERC) and the Government of Ontario for an Early Career Research Award to EIA.

Notes and references

1 M. Griffith, K. I. Udekwu, S. Gkotzis, T. F. Mah and E. I. Alarcon, in *Silver Nanoparticle Application*, ed. E. I. Alarcon, M. Griffith and K. Udekwu, Engineering Materials, Springer, Cham, 2015, pp. 127–146.
2 J. S. Kim, E. Kuk, K. N. Yu, J.-H. Kim, S. J. Park, H. J. Lee, S. H. Kim, Y. K. Park, Y. H. Park, C.-Y. Hwang, Y.-K. Kim, Y.-S. Lee, D. H. Jeong and M.-H. Cho, *Nanomedicine*, 2007, **3**, 95–101.
3 K. K. Wong, S. O. Cheung, L. Huang, J. Niu, C. Tao, C. M. Ho, C. M. Che and P. K. Tam, *ChemMedChem*, 2009, **4**, 1129–1135.
4 Z. Khatoon, C. D. McTiernan, E. J. Suuronen, T.-F. Mah and E. I. Alarcon, *Heliyon*, 2018, **4**, e01067.
5 K. Markowska, A. M. Grudniak and K. I. Wolska, *Acta Biochim. Pol.*, 2013, **60**, 523–530.
6 S. Pal, Y. K. Tak and J. M. Song, *Appl. Environ. Microbiol.*, 2007, **73**, 1712.
7 M. Rai, K. Kon, A. Ingle, N. Duran, S. Galdiero and M. Galdiero, *Appl. Microbiol. Biotechnol.*, 2014, **98**, 1951–1961.
8 X. Lu, P. Xu, H.-M. Ding, Y.-S. Yu, D. Huo and Y.-Q. Ma, *Nat. Commun.*, 2019, **10**, 4520.
9 C. Corbo, R. Molinaro, A. Parodi, N. E. Toledano Furman, F. Salvatore and E. Tasciotti, *Nanomedicine*, 2016, **11**, 81–100.
10 N. Durán, C. P. Silveira, M. Durán and D. S. T. Martinez, *J. Nanobiotechnol.*, 2015, **13**, 55.
11 M. Ahumada, C. Bohne, J. Oake and E. I. Alarcon, *Chem. Commun.*, 2018, **54**, 4724–4727.
12 K. P. Shay, R. F. Moreau, E. J. Smith, A. R. Smith and T. M. Hagen, *Biochim. Biophys. Acta*, 2009, **1790**, 1149–1160.
13 S. Simoncelli, H. de Alwis Weerasekera, C. Fasciani, C. N. Boddy, P. F. Aramendia, E. I. Alarcon and J. C. Scaiano, *J. Phys. Chem. Lett.*, 2015, **6**, 1499–1503.
14 *Nanoparticle Technology Handbook*, ed. M. Hosokawa, K. Nogi, M. Naito and T. Yokoyama, Elsevier, Amsterdam, 2008, pp. 593–596.
15 A. H. Pakiari and Z. Jamshidi, *J. Phys. Chem. A*, 2010, **114**, 9212–9221.
16 G. C. Cotton, C. Gee, A. Jude, W. J. Duncan, D. Abdelmoneim and D. E. Coates, *RSC Adv.*, 2019, **9**, 6973–6985.
17 C. Dumas and C. J. Meledandri, *Langmuir*, 2015, **31**, 7193–7203.
18 O. Horovitz, M. Tomoaia-Cotisel, C. s. Racz, G. Tomoaia, L. D. Boboș and A. Mocanu, *Stud. Univ. Babes-Bolyai, Chem.*, 2009, **54**, 89–96.
19 K. Niska, N. Knap, A. Kedzia, M. Jaskiewicz, W. Kamysz and I. Inkielewicz-Stepniak, *Int. J. Med. Sci.*, 2016, **13**, 772–782.
20 K. Teeparuksapun, N. Prasongchan and A. Thawonsuwan, *Anal. Sci.*, 2019, **35**, 371–377.
21 S. K. Vaishnav, K. Patel, K. Chandraker, J. Korram, R. Nagwanshi, K. K. Ghosh and M. L. Satnami, *Spectrochim. Acta, Part A*, 2017, **179**, 155–162.
22 S. Berchmans, P. J. Thomas and C. N. R. Rao, *J. Phys. Chem. B*, 2002, **106**, 4647–4651.

23 K. Chandraker, S. K. Vaishanav, R. Nagwanshi and M. L. Satnami, *J. Chem. Sci.*, 2015, **127**, 2183–2191.
24 J. Jiménez-Lamana and V. I. Slaveykova, *Sci. Total Environ.*, 2016, **573**, 946–953.
25 M. A. Lebda, K. M. Sadek, H. G. Tohamy, T. K. Abouzed, M. Shukry, M. Umezawa and Y. S. El-Sayed, *Life Sci.*, 2018, **212**, 251–260.
26 K. Ngamchuea, C. Batchelor-McAuley and R. G. Compton, *Nanotoxicology*, 2018, **12**, 305–311.
27 L. Ramachandran and C. K. K. Nair, *Nanomater. Nanotechnol.*, 2011, **1**, 14.
28 H. S. Toh, K. Jurkschat and R. G. Compton, *Chem.–Eur. J.*, 2015, **21**, 2998–3004.
29 M. J. Davies, *Biochem. J.*, 2016, **473**, 805–825.
30 E. Niki, *Methods Enzymol.*, 1990, **186**, 100–108.

